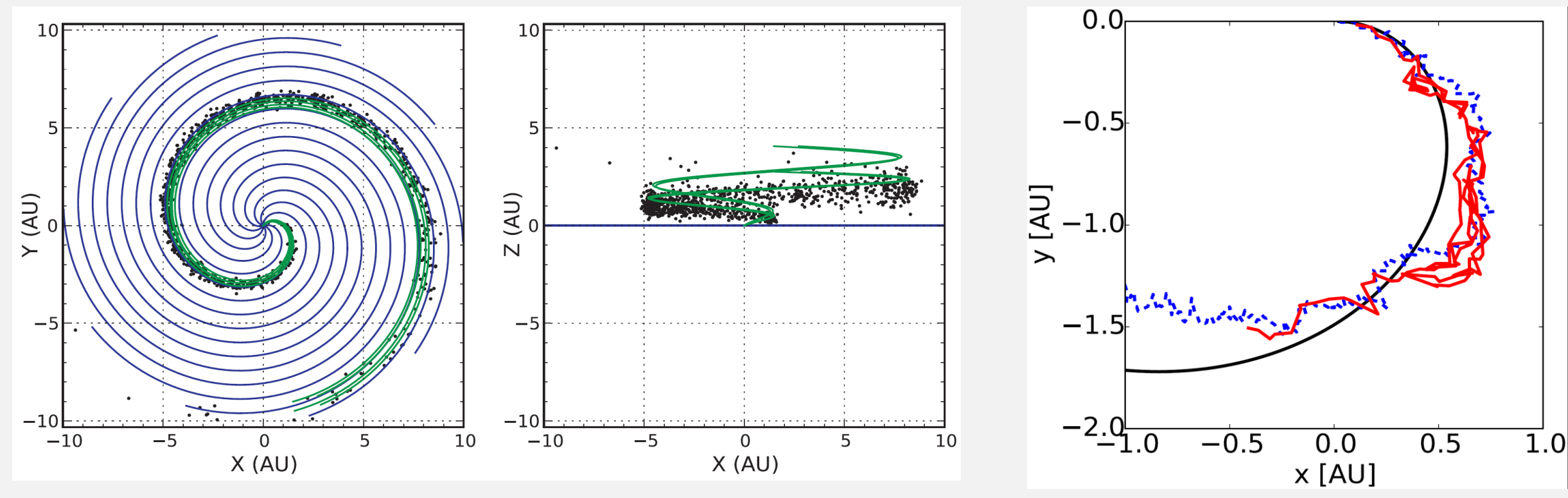


EFFECT OF LARGE-SCALE DRIFTS ON SEP PROPAGATION ALONG TURBULENT MAGNETIC FIELD LINES

T. LAITINEN, S. DALLA
JEREMIAH HORROCKS INSTITUTE, UNIVERSITY OF CENTRAL LANCASHIRE, UK

1 Introduction



Particles (black symbols) drifting from initial Parker spiral magnetic field lines (green curves) (Marsh+ 2013)

Particle (solid red) following turbulent fieldline (dashed blue) that meanders about the Parker spiral (thick black) (Laitinen+ 2016)

Solar Energetic Particles (SEPs) are accelerated during solar eruptions, and propagate in interplanetary space before being observed in situ. Their propagation is modulated by turbulent magnetic field (e.g. Parker 1965) and the large-scale magnetic field structure.

In addition to propagating along the Parker Spiral field lines, the SEPs drift across the mean field due to large-scale curvature and gradients of the heliospheric magnetic field (top left panel) (Dalla et al 2013). The particles also decelerate as they drift across the convective $\mathbf{V}_{sw} \times \mathbf{B}$ electric field, which lies in the latitudinal direction in the standard Parker spiral configuration (Dalla et al 2015). Further, the particles drift along the heliospheric current sheet.

The turbulence on the other hand causes the field lines to random-walk, and the particle propagation is guided by this stochastic meandering (Laitinen et al 2013, 2016). The propagation of the SEPs is initially deterministic along the stochastically meandering fieldlines (top right), and at later times can be described as diffusion across the mean magnetic field (e.g. Jokipii 1966).

The combined effect of the drift and the turbulent random-walk of fieldlines on the particle propagation has so far been considered only at the asymptotic diffusion limit, where strong turbulence can suppress the large scale drifts (e.g. Giacalone et al 1999, Minnie et al 2007). However, these studies employ time-scales and turbulence levels high for SEP propagation. Also, the influence of the drifts to the stochastic spreading of the particles has not been addressed.

In this work we investigate the combined effect of drifts and fieldline meandering on SEP propagation, in particular the effect of the drifts on the spreading of the particle population in across the field.

2 Model for drifts and turbulence

We employ a simple magnetic turbulence model with a constant background magnetic field B_0 along z-axis, superposed with transverse slab and 2D Fourier modes to depict turbulence:

$$\mathbf{B}(x, y, z) = B_0 \hat{\mathbf{e}}_z + \delta \mathbf{B}_{2D}(x, y) + \delta \mathbf{B}_{slab}(z)$$

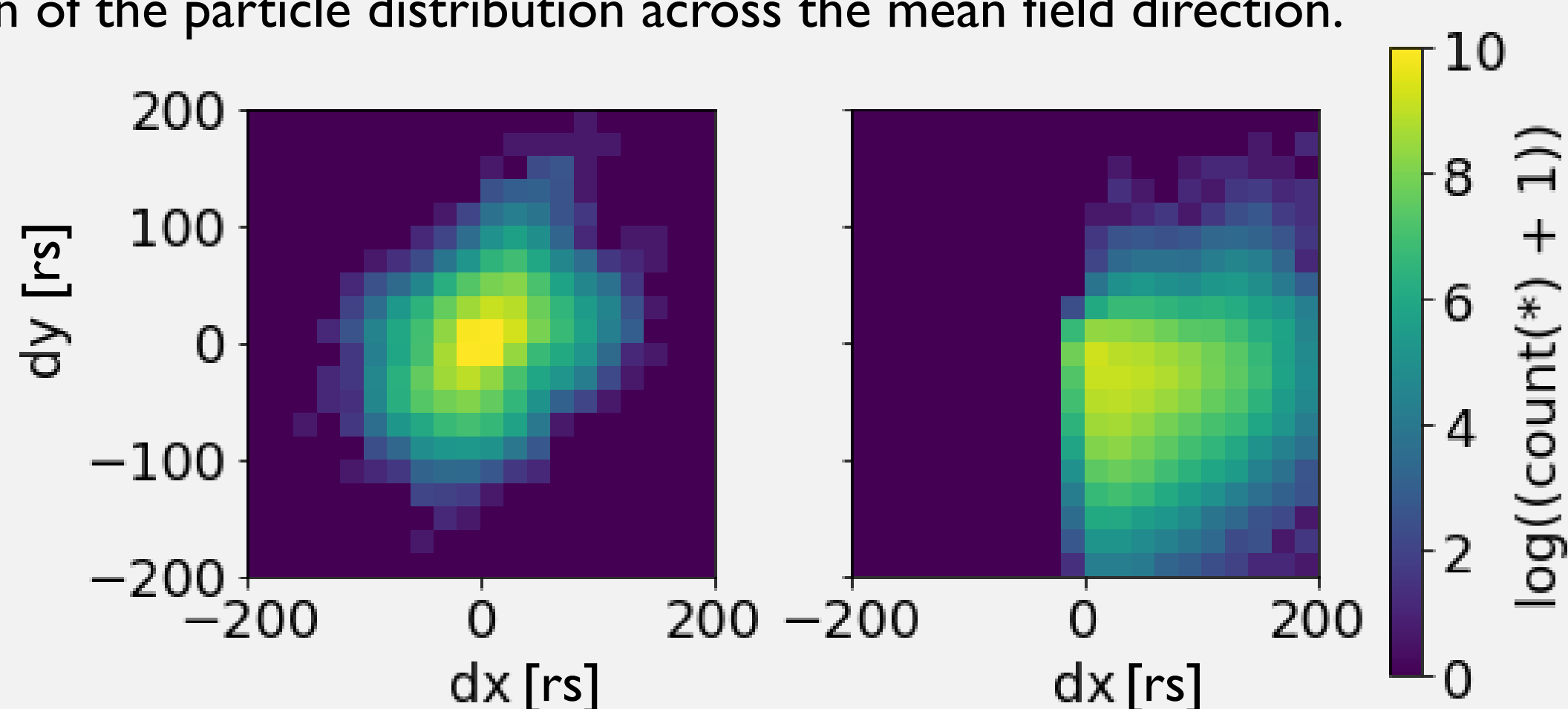
With $\delta \mathbf{B}_{2D} \perp \hat{\mathbf{e}}_z$ and $\delta \mathbf{B}_{slab} \perp \hat{\mathbf{e}}_z$, and $B_0 = 50 \mu\text{G}$ consistent with field at 1 AU.

To facilitate the large-scale drifts, we add an electric field $\mathbf{E} = E_0 \hat{\mathbf{e}}_x$ which will result in $\mathbf{v}_E = c \mathbf{E} \times \mathbf{B} / B^2$ drift mainly in the negative y direction. We use $E_0 = 10^{-7}$ statvolt/cm, which is on the upper scale of reasonable values in the heliosphere, and reasonable upper limit of heliospheric drift velocity magnitudes.

We solve the full equation of motion

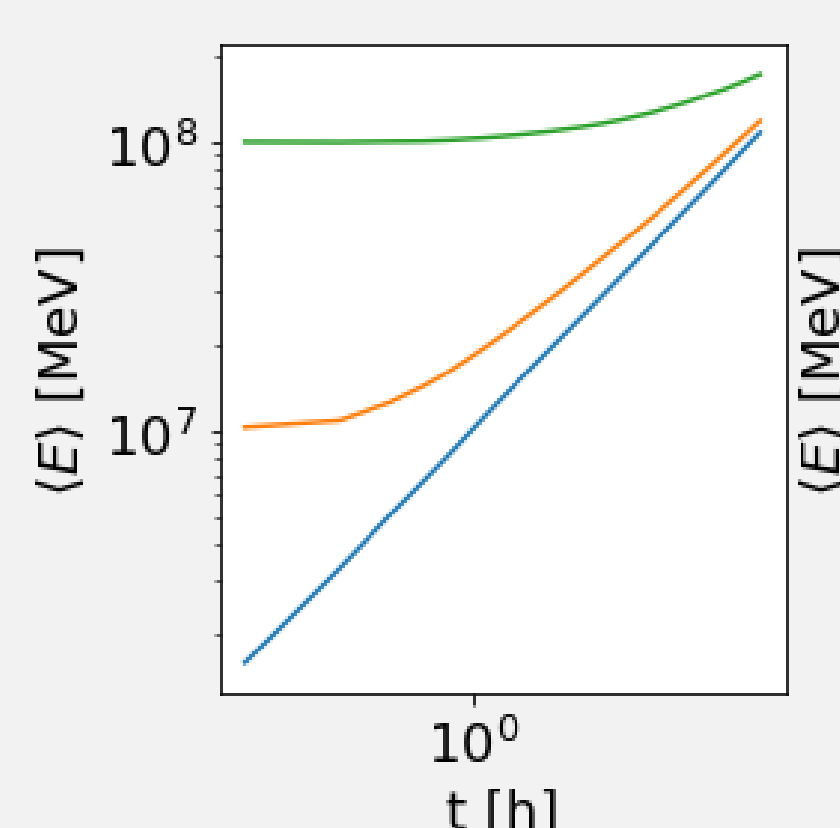
$$\frac{d\mathbf{p}}{dt} = q \left(\mathbf{E} + \frac{\mathbf{v}}{c} \times \mathbf{B} \right)$$

for 10 MeV protons with isotropic initial velocity distribution to analyse the evolution of the particle distribution across the mean field direction.



The contours above show the 10-MeV proton distribution across the mean field direction after 21 hours simulation time for the cases with $E_0 = 0$ and $E_0 = 10^{-7}$ statvolt/cm for left and right contours, respectively. In the right contour, the population has drifted along negative y direction, due to the $\mathbf{E} \times \mathbf{B}$ drift. The population has drifted also along positive x direction. This is due to the particles accelerating as they propagate across the mean magnetic field, along the electric field while following the meandering field lines.

The evolution of the mean energy is shown in the right panel for three different initial energies 1, 10 and 100 MeV. The contours show also a large-scale skew that is due to the scale skew in the realisation of the turbulence field. The skew varies from realisation to realisation.

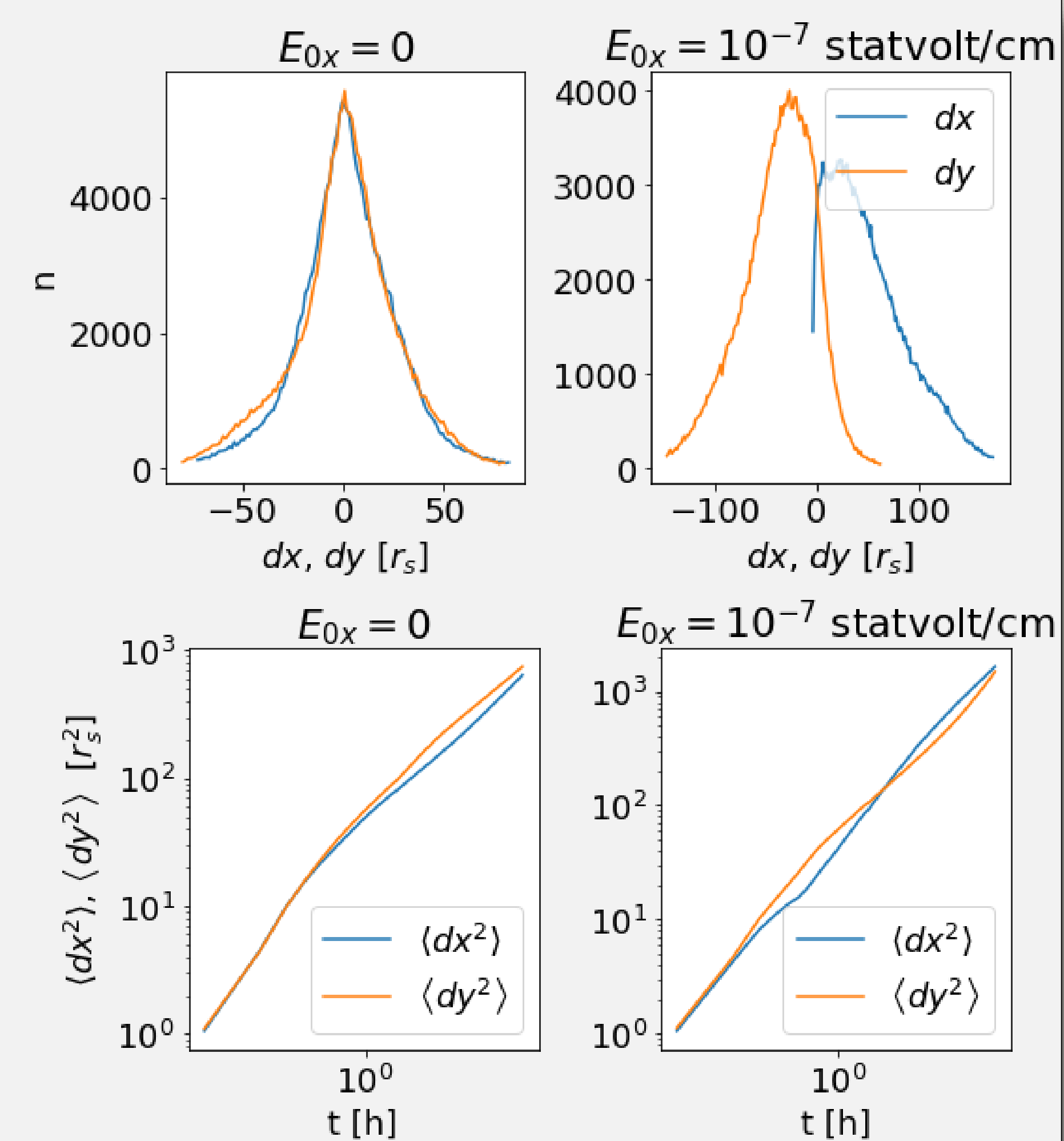


3 Distribution of all particles

In the top panel we show distribution of 10 MeV protons across the mean field direction after 21 hours, with blue and orange curves showing distribution along electric and drift direction, respectively. Here, all particles are included in the distribution irrespective of their location along the mean field direction.

In left panel, the electric field is zero and the distributions are identical. However, on the right, with a non-zero electric field in x-direction, the distribution drifts and is skewed to negative y, whereas the x-distribution has drifted and is skewed towards positive x.

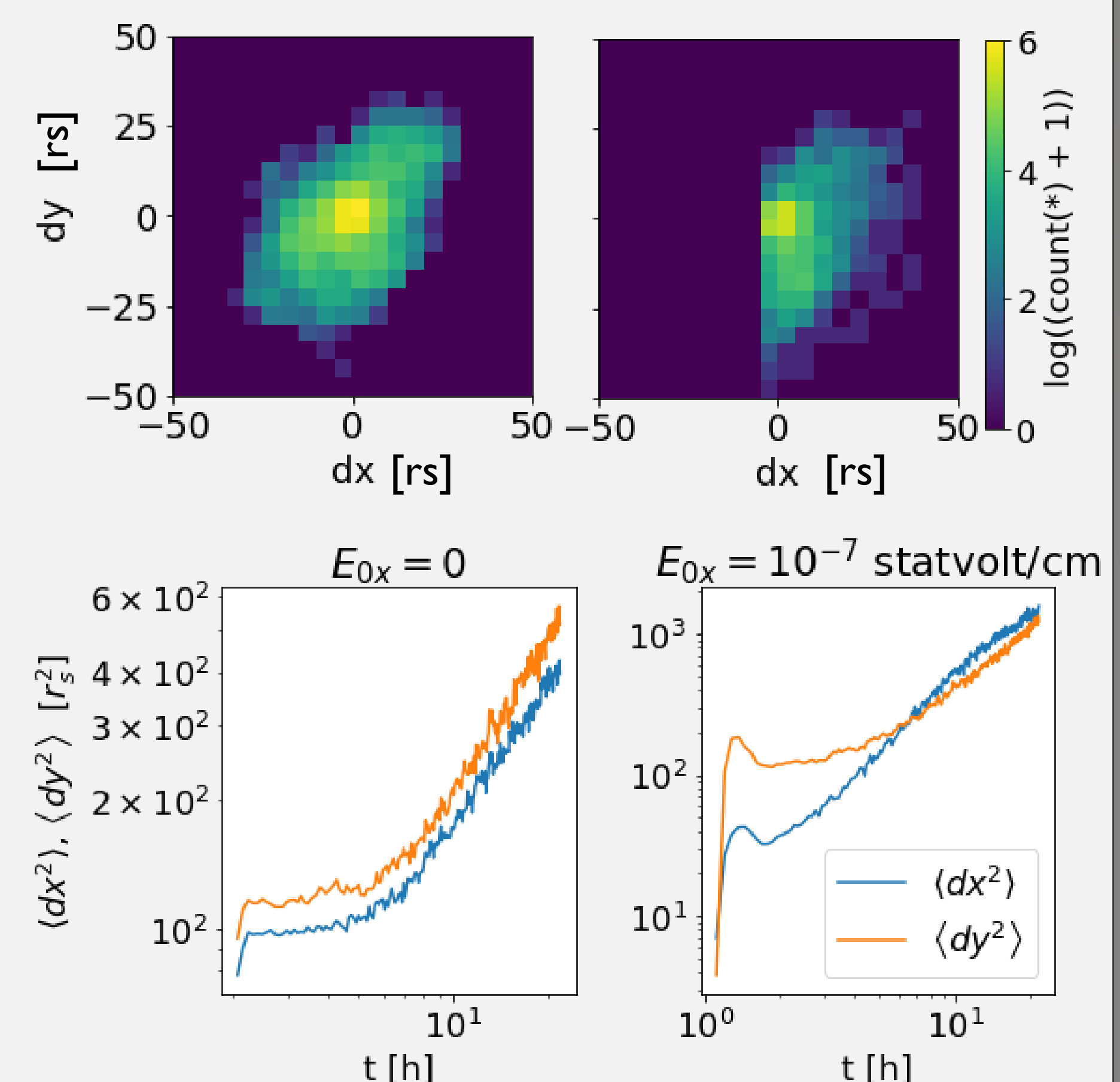
In the bottom panel, we show the evolution of the cross-field variance of the particle distribution in time. The comparison of the curves shows that the electric field results in wider spread of particles across the field. However, spread is similar in the two directions.



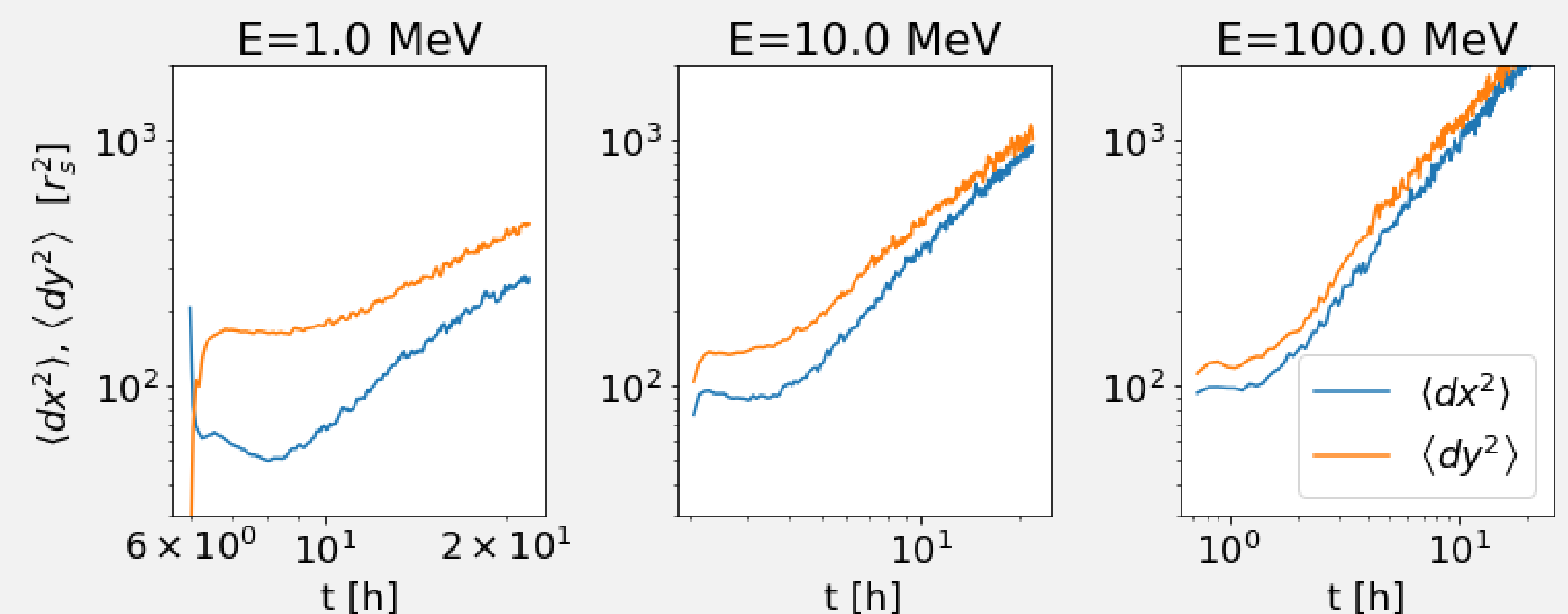
4 Distribution of particles at 1 AU

In the panels on the right, we show the distribution of particles as they cross 1 AU distance from their origin. On the top, we show the distribution of particles 2 hours after injection. We again see that the electric field (right panel) causes drifting and additional spread of particles in negative y-direction due to drift, and positive x-direction due to acceleration.

Bottom panel shows the evolution of the variance width of particle distribution at 1 AU. We see that the $\mathbf{E} \times \mathbf{B}$ drift causes initially slightly faster spread of particles in the y-direction. The initial spreading in x-direction is slower in the case of electric field, which may be due to interplay between acceleration and scattering. Subsequently the spread of particles in x-direction overtakes that in y-direction. This may be caused by the acceleration of particles along the electric field.



5 Distribution of particles at 1 AU: excluding acceleration



In the panels above, we have modified the large-scale electric field so that $\mathbf{E} \cdot (\mathbf{B}_0 + \delta \mathbf{B}) = 0$ to prevent the acceleration of particles as they propagate along meandering fields. We find that the difference between the variance along and across the electric field is diminished, however still present at lower energies. Further work is needed to establish the significance of the difference as compared to variation due to turbulence realisation differences.

6 Conclusions

- SEP propagation across the mean magnetic field depends on both large-scale drifts and field-line meandering due to turbulence.
- Particles gain and lose energy as they propagate along the electric field due to meandering of fieldlines. This implies latitude-dependence for particle energy spectra seen also due to drifts alone (Dalla et al 2020).
- Coupling of the energy changes and the $\mathbf{E} \times \mathbf{B}$ drift result in complex evolution of the particle distribution of particles across the mean field direction at 1 AU along the electric field and $\mathbf{E} \times \mathbf{B}$ drift directions.
- Removing acceleration due to the electric field, the coupling between drifts and fieldline meandering still results in different spreading of particles along the field and drift directions at low energies.

Acknowledgements

We acknowledge support from STFC (grant ST/R000425/1). This work was performed using resources provided by the Cambridge Service for Data Driven Discovery (CSD3) operated by the University of Cambridge Research Computing Service (STFC capital grant EP/P020259/1) and DIRAC funding from the STFC. Access to the University of Central Lancashire's High Performance Computing Facility is gratefully acknowledged.

References

- Dalla, S., Marsh, M. S., Kelly, J., & Laitinen, T. (2013). *JGR*, 118, 5979.
- Dalla, S., Marsh, M. S., & Laitinen, T. (2015). *ApJ*, 808(1), 62.
- Dalla, S., Nolfo, G. A. de, Bruno, A., Giacalone, J., Laitinen, T., Thomas, S., Battarbee, M., & Marsh, M. S. (2020). *A&A*, 639, A105.
- Jokipii, J.R. (1966). *ApJ*, 146, 480.
- Giacalone, J., Jokipii, J.R., & Kóta, J. (1999). *ICRC*, 7, 37.
- Laitinen, T., Dalla, S., & Marsh, M. S. (2013). *ApJL*, 773(2), L29.
- Laitinen, T., Kopp, A., Effenberger, F., Dalla, S., & Marsh, M. S. (2016). *A&A*, 591, A18.
- Marsh, M. S., Dalla, S., Kelly, J., & Laitinen, T. (2013). *ApJ*, 774(1), 4.
- Minnie, J., Bieber, J.W., Matthaeus, W.H., & Burger, R.A. (2007). *ApJ*, 670(2), 1149.
- Parker, E. N. (1965). *Planet. Space Sci.*, 13(1), 9–49.